T. Z. Martin

Spatial Variability in the Seasonal South Polar Cap of Mars

Wendy M. Calvin.* and Terry Z. Martin[2]

Manuscript submitted to JGR-Planets

Draft Version November 15, 1993

Number of pages: 19

Number of tables: 1

Number of figures: 12

[1]U.S.G. S.-Branch of Astrogeology, 2255 N Gemini Dr, Flagstaff, AZ 86001
[2]JPLMS 169-237, 4800 Oak Grove Dr., Pasadena. CA 91109

Address correspondence to:

Dr. Wendy M. Calvin

U. S. Geological Survey

Branch of Astrogeology

2255 North Gemini Drive

Flagstaff, AZ 86001

Tele: (602) 556703.5

FAX:(602) 1556701.1

internet:wcalvin@hulk.wr.usgs.gov

Suggested Running Head:

Variation in the Martian South Polar Cap

ABSTRACT

We present the first comprehensive discussion of the south seasonal polar cap spectra obtained by the Mariner 7 Infrared Spectrometer in the short wavelength region (2–4 μm). In addition we correlate the infrared spectra with images acquired by the wide angle camera, Significant spectral variation is noted in the cap interior and regions of varying water frost abundance, CO_2 ice/frost cover. and CO_2-ice path length can be distinguished. Many of these spectral variations correlate with heterogeneity noted in the camera images but certain significant infrared spectral variations are not discernible in the visible. We use simple reflectance models to classify the observed spectral variations into four regions. Region I is at the cap edge where there is enhanced absorption beyond 3 μm inferred to be caused by an increased abundance of water frost. The increase in water abundance over that in the interior is on the level of a few parts per thousand or less, Region 11 is the typical cap interior characterized by spectra] features of CO_2 ice at grain sizes of several millimeters to centimeters, These spectra also indicate the presence of Water frost at the parts per thousand level. .4 third, unusual region (III), is defined by three spectra in which weak CO_2 absorption features are as much as twice as strong as in the average cap spectra and are assumed to be caused by an increased path length in the CO_2. The final region (IV) is an area of thinning frost coverage or transparent ice well in the interior of the seasonal cap. These spectra are a combination of CO_2 and ground signatures.

I Introduction/Data Set

The Mariner 7 spacecraft flew by Mars on August 5, 1969 (L_s 2000). The set of spectra obtained by the IR Spectrometer (IRS) covered primarily southern equatorial latitudes! with one strip extending from about -4.5 to -75°. Spectra covering the range 1.9- 14.4 μm with 1-2% resolution were acquired using circular variable interference filters. Although the flyby occurred in 1969, there has never been a detailed discussion of the spatial variation of the spectra acquired over the polar cap. Herr and Pimentel (1969) identified diagnostic absorption at 3.0 and 3.3 μm as being caused by solid CO_2. Laboratory measurements by Kieffer (1 970) and observations by Larson and Fink (1972) demonstrated that weak absorption at 2.28 and 2.34 μm are characteristic. of forbidden transitions in solid $C0_2$. All four of these absorption are clearly seen in the Mariner 7 polar cap spectra and it was noted that these features disappear in the most poleward spectra (Herr and Pimentel. 1969 and Pimentel *et al.*, 1974). In addition to the general poleward disappearance, both Martin (1988) and Calvin (1990) noted that the weak bands at 2.2S and 2.34 pm exhibit variability with location in the cap and Calvin (1990) show-cd that these bands are sensitive indicators of grain size. Pimentel *et al.* (1974) also noted, based upon intensity ratios, that there was likely a collar region of water ice,

The advent of a variety of theoretical models for calculating reflectance and albedo. coupled with the compilation of optical constants for solid $C0_2$ by Warren (1986), led both Warren *et al.* (1990) and Calvin (1990) to explore reflectance variations of solid $C0_2$ as a function of grain size. in addition, Warren *et al.* (1990) examined the effects of water and dust contamination and found that water would have a significant impact on therms] emissivity but little effect on the albedo. while dust would strongly affect the al bedo. Calvin (1990) noted that the 2.3 μm bands in the Mariner spectra are most similar to coarse-grained laboratory frosts. However, both of these 1990 studies were ultimately limited by the accuracy of the optical constants of CO_2.

Recently, a more accurate determination of the optical constants of solid CO_2 (Hansen, 1992) allows us to take a more comprehensive approach to characterizing both the individual spectra acquired by Mariner 7 as well as spectral variations within the cap. In addition we correlate the

infrared spectra with images acquired by the Mariner wide angle camera. Many spectral variations correlate with spatial changes in the camera images but certain significant spectral variations are not discernible in these pictures. In particular, the use of the camera images leads to a new interpretation for the disappearance of the CO_2 features in the most poleward spectra.

The data set, originally archived on microfiche, was restored by Martin (1985) in raw digital form. More recently, a full restoration to radiance and wavelength has been performed (Martin, 1993). For the polar regions. the most diagnostic spectral variations occur in the short wavelength segment. 1.9–3.7 μm. At the longer wavelengths the transition from frost-free to frosted areas is noted but the spectral signature is dominated by the warm atmosphere above the cold cap. As there is little variation in the spectral segments from 4–14.5 μm only spectra of the shortest wavelength segment are presented here.

Absolute radiometric calibration remains problematic for this short wavelength segment (Martin, 1993). Strong slopes from 1.9 to 2.7 μm are introduced in both off and on cap spectra that do not agree with ground based telescopic observations (Roush *et al.*, 1992). For these reasons we use the raw spectra corrected for wavelength and the cosine of the incidence angle (cos(i)) and examine relative variation among the spectra, Models are presented to show trends rather than to achieve a precise match to the Mariner spectra. Figure 1 demonstrates the difference between the raw, cos(i) correction and the radiometric correction. Aside from the strong slope in the continuum level from 1.9-2.6 μm in the radiometrically corrected spectrum, the two are very similar. In particular, the reflectance level beyond 3 μm varies only about 5% between the two. This point will be important for following arguments regarding the presence of water frost.

We examine 29 spectra of the seasonal south cap including a few off-cap ground spectra. Here and elsewhere in this paper we use the term ground to refer to the "dirt" surface, i.e. with no apparent condensate. These spectra were acquired from -54.1°, 32.9° (lat,lon), across the southern regions of Noachis Terra, through South and Main craters to -77.6°, 299.3°. The next section describes variations among the 29 spectra followed by a discussion of the implications of theoretical models for water frost abundance and path lengths in the $C0_2$ ice.

II Visual and Spectral Variation

The spatial coverage of the IRS is shown in Fig. 2, where footprints of selected observations have been overlaid on Mariner 7 TV camera images of the cap edge and interior. In order to perform this registration, the latitude/longitude coordinates supplied by the Project in 1969 for the IRS slit endpoints were put over images projected on a lat/lon grid. Note that the coordinate system used then is different from that adopted after Mariner 9 in 1971. The lat/lon coordinates given here for individual spectra are in the current coordinate system. The images shown here are versions processed to preserve albedo information. It is evident how frost coverage increases across the cap edge, and that significant albedo variation exists within the cap interior.

A surface plot of the polar cap spectra is presented in Fig. 3. Each line of the mesh parallel to the wavelength axis represents a single observation. Mesh lines in the other direction are surfaces of constant wavelength. Absorption features appear as grooves or dips in the surface. The four regions that we classify in the following discussion are labeled in reman numerals. These regions are grouped by increasing spectrum number. which roughly corresponds to more poleward latitudes. The atmospheric absorption from 2.7-2.8 μm can be clearly seen as a trough at the approximate center of the surface. The 3.1 and 3.3 μm $C0_2$ absorption can be noted in sections I through III, and are seen to almost disappear in section IV. The cap edge is clearly seen by the ramp up in signal level in the 2.1–2,.5 μm region. The 2.28, 2.34, and 2.42 μm absorption features appear as depressions in the high plateau on the left. Six spectra (120, 126, 132. 138, 144, and 1.50) are missing from the digital data set; these were the spectra acquired through a polystyrene filter to assist in wavelength calibration, The periodic dips at the shortest wavelengths are an artifact of the polystyrene filter and occur just before each missing spectrum.

Figure 4 shows spectral plots of individual observations selected from throughout the cap, These demonstrate the general trends observed in Fig. 3 and further clarify the four regions in the cap based upon similarities or differences in the infrared spectra. Also refer to Figs. 2 and 3 for the following discussion. First note the increasing albedo from 2.2-2.5 μm in the transition from frost-free to frosted areas, spectra 119 to 127, with a typical frost free spectrum 122 shown in Fig.

4. Region I at the cap edge is defined by the decreased albedo beyond 3 μm. This area is covered by spectra 1'27-130 with spectrum 130 shown in Fig. 4a. The part of these spectra attributable to condensates is the same as in the interior (131 to 142) except for the lower 3 μm level. Region II is the typical interior with spectra 134 and 136 shown in Fig. 4. The third region (111) appears most spectacularly in the individual plots and is distinguished by the enhanced strength of the 2.3 μm absorption and an associated low 3 μm reflectance. Spectrum 145 is shown in Fig. 4b, and 143 to 146 span this anomaly. The depression of the wavelengths beyond 3 μm can also be seen in the surface plot in Fig. 3. Finally, the spectra farthest south (147 to 153) (IV) show decreased reflectance levels and suppressed CO_2 features, Spectrum 151 is the representative shown in lig. 4b.

Region III is characterized by very unusual spectra and is localized in space. so we examine it in closer detail. This area is primarily distinguished by the enhanced band depth of the CO_2 features near 2,3 μm. Figure 5 shows the band depth of the 2.28 μm feature as a function of spectrum number. There is a smooth transition in band depth from the average interior into the anomalous region surrounding spectrum 145. centered on -7.5.5°, 338.6° (lat,lon). This region is the northwest flank of South crater, but surprisingly, there is no variation noted in the wide angle camera images in Fig. 2b. It should also be noted that in spite of the drastic change in the 2.3 μm band depths, the level near 2.2 μm remains almost unchanged.

As noted by Calvin (1990) and Calvin *et al.* (1993a) the absorption near 2.3 μm are quite strong throughout the cap with an average depth near 7'% (Fig. 5). This is typical of lab frosts with grain sizes on the order of millimeters (Kieffer, 1970; Calvin, 1990). Other seasonal south cap observations also show strong absorption in these bands. Larson and Fink (1972) observed at L_s 200" in 1971 and noted that the 2.3 μm features and other weak features were best matched by a CO_2 ice surface while strong features were best fit by finer-grained frosts. Clark *et al.* (1990) presented data from near L_s 260° in 1988 which showed band depths of 10% for the 2.3 μm features. Their spectral resolution was better than the IRS, leading to deeper absorption features, but their data are consistent with other observations. The maximum 16% depth of these features in the M7

spectrum 145 may be characteristic of CO_2 ices with grain sizes on the order of tens of centimeters. The next section on model calculations discusses this possibility in greater detail.

An additional spectral feature of the region around spectrum 145 is enhanced absorption beyond 3 μm. We have found the ratio of intensities at 3.1/2.2 μm to be diagnostic of this absorption: a plot of this ratio is shown in Fig. 6. 'There are two areas associated with enhanced 3 μm absorption, one at the cap edge, Region 1, and one associated with the maximum 2.3 μm band depths of spectrum 145.

The fourth region is defined by the disappearance of the diagnostic CO_2 absorption features in the most poleward spectra. Herr and Pimentel (1969) discussed this disappearance and suggested particle size effects or impurities, as there were no clouds or atmospheric. effects to account for the loss. Calvin (1990) suggested that either impurities or extremely large grain sizes in CO_2 ice could lead to the suppression of features. Referring to the camera image in Fig. 2b, we clearly see the expression of ground features indicating either a thinning coverage or increased transparency of the overlying CO_2. Either of these conditions yields a spectrum that is a combination of the ground and CO_2 spectra. The next section on models discusses the effectiveness of a ground signature in suppressing CO_2 features. An additional diagnostic is the ratio of intensities at 2,6,5/2.2 μm. This ratio is shown in Fig. 7 and is indicative of the appearance of a ground signature in both frost free regions north of the seasonal cap edge and in the cap interior. In Fig. 7, the first few ground spectra have high ratios and the value dips below 0.2 at spectrum number 128, where there is near full CO_2 ice coverage. For the last six or seven spectra the ratio, while low, is again above the 0.2 value indicating the presence of a ground contribution to the spectra. This effect can also be seen in the surface plot of Fig. 3 as a ridge of varying height just to the left of the 2.7 atmospheric absorption bands.

We summarize the four spectrally distinct regions in the seasonal cap and in the next section apply theoretical models to estimate grain sizes and the level of water or dust contamination.

Region 1: There is an enhancement at the cap edge in absorption beyond 3 μm. [127--130)

Region II: Average interior spectra are characterized by large 2.3 μm band depths. (131-142)

Region III: There is a unique spot where the 2.3 pm bands are over twice as deep as the average and tile reflectance beyond 3 μm is suppressed, This spot has no obvious visual expression in the camera images and the level at 2,2 μm remains high. (143, 145, 146)

Region IV: The most poleward spectra show a rise in reflectance level at 2.6 pm, and a disappearance of typical solid CO_2 absorption bands corresponding to the appearance of ground features in the camera images. (147-153)

III Theoretical Models

Following the approach of Calvin (1990) we use Hapke (1981) theory for calculating CO_2 reflectances. The optical constants of C'0, were obtained from Warren (1986) and Hansen (1992). The imaginary index from Hansen (1992) shows a broad triangular feature from approximately 2.9 to 3,2 μm that is caused by contamination at the parts per million (ppm) level by H_20. Water has an absorption coefficient that is an order of magnitude greater than that of CO_2 at this wavelength so even small quantities can have a significant effect. Similar effects were seen in the lab spectra of Ditteon and Kieffer (1979) and were shown by Calvin (1990) to be a potential water contamination problem. As no other laboratory CO_2 frost or ice spectra show this feature, we have adjusted the imaginary index values of Hansen (1992). This was accomplished by first converting his imaginary index to an absorption coefficient (cm^{-1}) and then scaling the values of Calvin (1990) to match those of Hansen and substituting Calvin's values from 2.997 to 3,237 μm. This substitution results in calculated CO_2 reflectance that are more similar to the Mariner observations in that they clearly show the 3.0 μm CO_2 feature.

To begin, we calculate reflectances of CO_2 as a function of grain size (Fig 8). These reflectance

were calculated at an average viewing geometry for the Mariner observation, 59° incidence angle, 43° emission angle, and 39° phase angle. Given the high incidence angles the calculated spectra snow higher reflectance values than typical laboratory observations, but the band depths are not affected. It was found, given the narrow nature of the CO_2 features, that a significant difference occurs depending on the order used when calculating reflectance and convolving to the Mariner 7 resolution. Fine structure in the 2 μm region noted in models of Calvin (1990) and not seen in the Mariner observations can be accounted for by her performing the convolution first. For the models here. all reflectance were calculated at the full resolution of the optical constants (typically better than 0.1 %) and then convolved to the Mariner 7 resolution (1.0-1.8% with an average near 1.6%).

Figure 9 shows the modeled depths of the 2.3 μm absorption features as a function of grain size. It is well known that atmospheric CO on Mars has a weak feature centered on 2.35 μm (e.g. Encrenaz and Lellouch, 1990). This can be expected to contribute approximately 0.5% to the band depth of the 2.34 μm CO_2 ice feature at Mariner 7 IRS resolution. We have corrected the modeled 2.34 μm band depth for atmospheric CO and plotted the range of typical values for the observed band depths. The average band depths observed by Mariner are equivalent to Hapke ices with grain diameters of 4 mm to 1 cm. The maximum 16% value of spectrum 145 is equivalent to 12 to 15 cm! Possible implications of these inferred grain sizes will be discussed later.

In comparing the calculated CO_2 reflectance with those observed by Mariner 7 we note that in the theoretical spectra the level beyond 2.9 μm returns to about 60% of the value between 2.2 and 2.5 μm. In the Mariner 7 spectra it is only about 30'% in both calibrated and uncalibrated data (Fig. 1). This indicates the presence of some contaminant which absorbs beyond 3 μm. Both water and dust are plausible and we next present some simple mixtures of CO_2 with H_2O and CO_2 with dust.

For the mixtures of CO_2 and H_2O the optical constants of H_2O ice from Warren (1984) were used. The dust constants were derived from an average of 3 ground spectra (1 19, 122, and 124) assuming a 50 μm grain size and an index of refraction from palagonite. Details of this type of inversion of a reflectance spectrum to attain absorption coefficients are given in Calvin (1990).

Models of CO_2/H_2O and CO_2/dust are presented in Fig. 10. The CO_2 grain size was 1 cm mixed with 0.1 to 0.5% of 50 μm grain H_2O. Figure 1011 is similar but with 0.1 to 5.0% dust. The spectra were calculated at the same viewing geometry as the pure CO_2 spectra in Fig. 8, then multiplied by a model martian atmosphere from Crisp (1990) convolved to Mariner resolution. Water is most effective at suppressing the region beyond 3 μm while retaining the 2.2 μm reflectance level. Dust impacts the overall reflectance level and suppresses the CO_2 features near 2.3, 3.0 and 3.3 μm. The inclusion of water introduces strong slopes in the spectral region from 2.2-2.5 μm that may or may not be consistent with the Mariner observations depending on the calibration. These spectral effects are also dependent on grain size but given the overall low abundance of water the grain sizes should not be much larger. Smaller water grains will brighten the reflectance below 2,6 μm, and suppress the region from 2.9-3.4 μm more.

We compare spectrum number 134 with the mixture of CO_2 and 0.2% H_20 in Fig. 11, The M7 data were approximately scaled to the reflectance value of the calculated spectrum. In general. the fit is quite good and small variations may be accounted for by the lack of intensity calibration. This fit suggests the average interior spectra may be best characterized by large grained CO_2 with some 11_20 at the parts per thousand (ppt) level. As the change in spectra from the cap edge (Region I) to the interior (Region 11) is strictly in the wavelength region beyond 3 μm, only small changes in water abundance are required to produce this effect. One way to examine the relative levels of H_2O is to ratio two spectra. In the ratio of spectra 130 to 134 the value in the 3 μm region is about 0.75 indicating that spectrum 130 with a lower level has more water. At the same time the ratio of the two spectra at 2.2 μm is approximately 1. The same ratio in calculated CO_2/H_2O mixes ranges from 0.7 to 0,83 in the 3 μm region. In a ratio of a calculated frost with 5ppt H_2O to one with 2ppt H_2O the value is 0.7 in the 3 μm region. For a calculated frost with 2ppt H_2O ratioed to lppt H_20 the value is 0,83. So variations of one to a few ppt 11_20 can produce the difference in reflectance in the 3 μm region observed from Region I to Region II spectra,

One difference between the observed and calculated spectra of Fig, 11 is the presence of an absorption feature at 2.42 μm observed in the Mariner spectra,. This feature is also seen in the

Clark *et al.* (1990) spectra and in the laboratory ice of Calvin (1990). It has been assumed that this absorption is caused by CO_2 based on analogy with large grained laboratory frosts (Calvin, 1990). The coefficients used for our calculations do not show' this absorption feature but in the most recent measurements of Hansen (1993, personal communication) CO_2 does show a weak absorption at this wavelength. However, in that measurement the 2,42 μm absorption is an order of magnitude smaller than the 2.2S and 2.35 μm absorption. In the M7, Clark *et al.* (1990), and Calvin (1 990) observations the 2.42 feature is only 2 to 4 times weaker than the 2,2S and 2.35 μm bands indicating possible enhancement of the 2.42 μm band on Mars and in coarse, grained laboratory ices. Although this feature is not apparent in the 2 mm frost of Kieffer (1970), it was observed to vary in laboratory $C0_2$ ices (unpublished data of WMC) and was strongest in the coarsest ices - those more like ice cubes than frosts. This suggests the feature may be enhanced by scattering and grain size effects in CO_2. Alternatively, there may be a coupling effect of a small amount of water in a carbon dioxide matrix which distorts the crystal structure and leads to a much stronger infrared transition. This potential effect is discussed further in the final section.

For both the cap edge transition Region I. and the interior Region IV, we found that simple linear mixtures of a typical Region II spectrum plus a ground spectrum were excellent matches (Fig. 12). For example, spectrum 148 can be fit extremely well by adding 55% of spectrum 134 with 45% of the average ground spectrum (119, 122 and 124). For the cap edge transition, these linear combinations were too high in the 3 μm region indicating the entire cap edge transition zone is enhanced in water over the typical interior. Figure 12 shows simple linear combinations for these two regions. Table 1 summarizes the unique spectral features of the individual spectra and gives the most likely interpretation based upon these simple models.

In Region III the 2.3 μm band depths are equivalent to calculated frosts with grain sizes of 12-15 cm but the 2.2 μm reflectance level remains high, Long paths or larger grains should lead to much lower reflectance levels overall. The high 2.2 μm level might suggest a finer $C0_2$ frost mixed with a coarser $C0_2$ ice. However. simple calculations of two different $C0_2$ grain sizes mixed are not, satisfactory at all. A reasonable spectral match may require more complex layered structures or

other factors that can enhance the weak features. The simple linear mixtures indicate that spectra on either side of the Region III anomaly have higher water abundances than the average cap interior (Table 1). Spectra 140, 141 and 142 all have more water than the average interior and 147 has an abundance equivalent to the cap edge. This suggests that at least part of the suppression beyond 3 μm in spectra 143, 145 and 146 is due to additional water frost as well as the increased CO_2 pathlength inferred from the extreme depths of the 2.3 μm absorption.

To summarize the general implications of simple reflectance models, we find that the equivalent grain sizes are large, with average grain sizes of a few millimeters to a centimeter consistent with Calvin (1990) and Calvin *et al.* (1993). A few spectra have potential grain sizes of 12 to 15 cm but we cannot model the region with simple mixtures and other effects may be creating the large band depths at 2.3 μm. There is some H_2O throughout the seasonal cap at the ppt level. There is an enhancement of H_2O a few ppt above the typical interior level, at the cap edge and at some spots in the interior, We see no evidence of pure H_2O frost but given the low abundances and large footprint we would not expect to. Subtle variations in the reflectance level in the 3 μm region can be a sensitive indicator of H_2O abundance and its spatial variation in the seasonal cap. At the most southern latitudes observed by Mariner 7 the seasonal CO_2 cap appears transparent or thinned so ground features contribute to spectral characteristics and suppress CO_2 ice absorption.

Albedo models by Hansen and Martin (1993 and personal communication) are consistent with our conclusions. Their models indicate that there is very little dust in spectrum 134 with H_2O/CO_2 ratios' from parts per million to parts per thousand. They find CO_2 grain sizes in the centimeter range and water grain sizes of 20 pm are the best fit. They also cannot duplicate the extreme band depths of spectrum 145.

IV Discussion

One of the most interesting results of this and other recent work is that the theoretical models are indicating equivalent grain sizes in the seasonal cap on the order of millimeters to centimeters, Given a possible value of 12 cm in the region around spectrum 14.5, it may be more appropriate to

talk of path lengths in the CO_2 cc surface. The seasonal cap in spring may be more like an ice cube with defects, rather than a snow pack with individual grains. Recent improvements to the optical constants of CO_2 between 1.8 and 2.4 μm (G.B. Hansen, personal communication) indicate that the model 2.28 and 2.34 μm band depths may be too strong. That is, even larger equivalent grain sizes may be required to match the observed band depths. If, however, scattering or other effects are enhancing the depth of these bands the present predictions of grain sizes should be the correct order of magnitude (1 to 10 centimeters). It seems unlikely that the seasonal cap will form with such large paths, so the grain sizes observed in southern spring are probably the result of metamorphism of the seasonal deposit over the winter. Eluszkiewicz (1993) has proposed a model for sintering of grains in the CO_2 seasonal cap that could yield long optical path lengths.

A remaining difficulty is a reasonable explanation for the anomalous spectra around South Crater and centered on -7.5.5°, 338.6° (lat,lon). The observing geometry is not strongly varying along the scan, and there is no evidence in the camera images of clouds. We believe this is a real surface effect, albeit one that has no expression at visible wavelengths. Indeed, the camera images are remarkably bland here. Given the inferred extreme path lengths required to produce the observed 2.3 μm band depths, the problem is then maintaining the reflectance level in the 2-2.5 μm region. Simple reflectance and albedo models are unable to reproduce the observed spectral characteristics. New theoretical models may be required which consider special problems associated with transmission and scattering in icy surfaces at high incidence angles. Herr and Pimentel (1969) commented that it was found in laboratory measurements of solid oxygen that forbidden transitions became allowed, and also varied greatly in strength, dependent on the deposition conditions. Thick samples and lattice imperfections resulted in significant band enhancement of normally weak or nonexistent features arising from forbidden traditions. This kind of process may also enhance the 2.42 μm absorption feature seen both in the seasonal Mars cap and in extremely coarse-grained laboratory CO_2 ices, The inferred increase in the abundance of water frost in this region suggests that the potential formation of clathrates within the $C0_2$ ice surface may also contribute to the large band depths of the 2.3 μm CO_2-ice features. Distortion of crystal structures resulting in new

or enhanced absorption features is not included in current, reflectance and albedo models.

It is expected that deposition or metamorphism conditions will vary spatially with solar insolation, local winds, cloud cover and other factors; all of these can contribute to the unique character of the seasonal cap on the northwest flank of South crater, It is interesting to note that this flank lies approximately in the lee of the crater from the prevailing spring and summer winds inferred by Thomas *et al.* (1979).

Emissivity of the cap depends strongly on both CO_2 grain size and the abundance of water frost (Warren *et al.*, 1990). Factors such as the transparency or thickness of the CO_2 ice deposit can also contribute to the thermal balance of the seasonal cap. Local variations in all these parameters are documented here, and are expected to contribute to the patchy and asymmetric recession of the seasonal south cap (e.g. James *et al.*, 1992 and references therein).

A recent comet model (Steiner and Kömle, 1993) indicates that a H_2O lag deposit develops rapidly in CO_2-H_2O mixtures. Given the overall low abundance of water on Mars this type of mechanism likely produces the observed enhancement of water at the cap edge where the insolation is highest and the cap sublimates most rapidly.

Given the inferred evolution of the seasonal cap with time and the strong coupling of the cap with the atmospheric $C0_2$ and H_20 cycles, further spectral monitoring of the cap is required. Telescopic observations are typically restricted to the southern spring and summer, so monitoring the seasonal evolution of the cap will require a spacecraft mission. The unfortunate loss of the Mars Observer Spacecraft is a setback to the accomplishement of that goal, but we remain optimistic that future Mars missions will fill in the gaps,

Acknowledgements

We wish to thank Gary Hansen for sharing his optical constants and many fruitful discussions regarding CO_2-H_2O models. The research by TZM was carried out at the Jet Propulsion Laboratory, California Institute of Technology, under a contract with the National Aeronautics and Space Administration. WMC was supported by the Mars Observer Thermal Emission Spectrometer project under a subcontract to the U. S. G. S. through Arizona State University.

REFERENCES

Calvin, W.M., 1990. Additions and corrections to the absorption coefficients of CO_2 ice: Applications to the martian south polar cap. *J. Geophys. Res.*, 95, 14743–14750.

Calvin, W.M., Martin, T. Z., and Hansen, G.B.,1993a, Spatial Variation in the seasonal south polar cap of Mars as observed by Mariner 7. *24th Lunar Planet. Sci. Conf.*, 2-13-244. [Abstract]

Clark, R. N., G. A. Swayze, R. B. Singer, and J. B. Pollack 1990. High-resolution reflectance spectra of Mars in the 2.3-μm region: Evidence for the mineral scapolite. *J. Geophys. Res.*, 95, 14463--14480.

Crisp, D. 1990. Infrared radiative transfer in the dust-free Martian atmosphere. *J. Geophys. Res.*, 95, 14577 -14.5S8.

Ditteon, 1{., and H. H. Kieffer 1979. Optical properties of solid $C0_2$: Application to Mars. *J. Geophys. Res.*. 84, 8294-8300.

Eluszkiewicz, J. 1993. On the microphysical state of the Martian seasonal caps. *Icarus*, 103, 43--1S.

Encrenaz, T., and E, Lellouch 1990. On the atmospheric origin of weak absorption features in the infrared spectrum of Mars. *J. Geophys.* Res., 95, 14589–14593.

Hansen, G. B. 1992. The spectral absorption of CO_2 ice from 0.18 to 4.S pm. *Bull. Am. Astron. Sot.*, 24, 978. [Abstract]

Hansen, G. B., and T, Z. Martin 1993. Modeling the reflectance of CO_2 frost with new optical constants: Application to Martian south polar cap spectra. *24th Lunar Planet. Sci. Conf.*, 601-602. [Abstract]

Hapke, B. 1981. Bidirectional reflectance spectroscopy 1. Theory. *J. Geophys. Res.*, 86, 303g-3054.

Herr, K. C.. and G. C. Pimentel 1969. Infrared absorption near three microns recorded over the polar cap of Mars. *Science*, 166, 496-499.

James, P. B., H. H. Kieffer, and D. A. Paige 1992. The seasonal cycle of carbon dioxide on Mars. In *Mars*, (H. H. Kieffer, B. M. Jakosky, C. W. Snyder, and M. S. Matthews, Eds.), pp. 934-968.

U. of Az Press, Tucson.

Kieffer, H. 11. 1970. Spectral reflectance of CO_2-H_2O frosts. *J. Geophys. Res.*, 75, 501-509.

Larson, II. 1'., and U. Fink 1972. Identification of carbon dioxide frost on the Martian polar caps. *Astrophys. J.*, 171, 1,91-1,95.

Martin. T.Z. 1985. Dataset restoration: The Mariner 6/7 infrared spectrometer. *Bull.* Amer. *Astron. Sot.*, 17, 723-724. [Abstract]

Martin, T.Z. 1988. Mariner 7 spectra of the Mars south polar CO_2 cap. *Bull. Amer. Astron. Sot., 20, 851.* [Abstract]

Martin, T. Z. 1993. Mariner 6/7 Infrared Spectrometer: Data set restoration. *J. Geophys. Rcs.* in press.

Pimentel, G. C., P. B. Forney, and K. C'. Herr 1974. Evidence about hydrate and solid water in the martian surface from the 1969 Mariner infrared spectrometer. *J. Geophys. Res.*, 79, 1623-1634.

Roush, 1. 1.., E. A. Roush, R. B. Singer, and P. G. Lucey 1992. Estimates of absolute flux and radiance factor of localized regions on Mars in the 2–4 μm wavelength region. *Icarus, 99, 42-.50.*

Steiner, G. and N. 1. Kömle 1993. Evolution of a porous 11_20 -CO_2–Ice sample in response to irradiation. J. *Geophys. Res., 98, 906.5-9073.*

Thomas, P., J. Veverka, and R. Campos-Marquetti 1979. Frost streaks in the south polar cap of Mars. *J. Geophys. Res., 84,* 4621-4633.

Warren, S. G, 1984. Optical constants of ice from the ultraviolet to the microwave. *Appl. Opt., 23, 1206-1225.*

Warren, S. G. 1986. Optical constants of carbon dioxide ice, *Appl. Opt., 25, 2650-2674.*

Warren, S. G., W. J. Wiscombe, and J, F. Firestone 1990. Spectral albedo and emissivity of CO_2 in Martian polar caps: Model results. *J. Geophys. Res., 95,* 14717-14741.

Table 1

Mariner 7 Polar Cap Spectra

Region	Observation Number	Description	Additional Comments
I	119-130	These spectra mark the transition onto the cap edge and are well modeled by simple linear combinations of typical interior (134) and average ground (119, 122, 124) spectra.	There is additional 3 μm suppression indicating a water frost abundance enhanced over that of the interior.
	119	Ground	
	121	Ground + 1% CO_2	
	122	Ground	
	123	Ground + 2% CO_2	
	124	Ground	
	125	Ground + 10% CO_2	
	127	55% CO_2 45% Ground	
	128	75% CO_2 25% Ground	
	129	85% CO_2 15% Ground	
	130	CO_2	
II	131-142	These are the typical cap interior spectra. They are similar to calculated frosts at 1cm grain size with the addition of 1 or 2 ppt water frost.	
	131	Slightly brighter than 134	Likely CO_2 grain size effect.
	133 - 137	Spectra are the same within noise level.	134 used as standard.
	139	Slightly lower reflectance overall.	Likely CO_2 grain size or dust effect.
	140, 141, 142	Spectra are the same within the noise level. Slightly lower 3 μm reflectance than 134.	More water than 134 but not as much as at the cap edge.
III	143, 145, 146	Unique region characterized by extremely large 2.3 μm band depths, 3 μm suppression, but levels at 2.2 μm unaffected.	2.3 μm bands equivalent to 12-15cm grain sizes but no model produces all spectral characteristics.
IV	147 - 153	Appearance of ground features in camera images. Spectra are well modeled by simple linear combination of typical interior (134) and average ground.	Minor additional water suppressing 3.0 and 3.3 μm CO_2 features. But typically below level at cap edge.
	147	85% CO_2	Water equivalent to cap edge.
	148	80% CO_2	
	149	75% CO_2	
	151	55% CO_2	Main crater.
	152	70% CO_2	
	153	70% CO_2	Water equivalent to cap edge.

FIGURE CAPTIONS

Figure 1: Spectrum number 134, corrected for viewing geometry (solid line) and the best radiometric correction (solid-dotted).

Figure 2: a) IR Spectrometer footprints plotted on Mariner 7 TV camera image 7N11, showing transition onto the south polar cap edge. IRS spectrum numbers are indicated. b) As in (a) but using camera image 7N 17, showing a region of anomalous spectral behavior centered at IRS spectrum number 145.

Figure 3: Surface plot of M7 spectra 119 to 153. See text for a complete description.

Figure 4: Selected spectra corrected for viewing geometry.

Figure 5: Band depth of the CO_2 feature at 2.28 μm.

Figure 6: Ratio of intensities at 3.1/2.2 μm. Low values differentiate the cap edge and the anomalous region surrounding spectrum number 145.

Figure 7: Ratio of intensities at 2.62/2.2 μm. Values above 0.2 are indicative of the presence of a ground signature in the spectra.

Figure S: Calculated reflectance of solid CO_2 as a function of grain size.

Figure 9: Band depths of the diagnostic 2.3 μm $C0_2$ features in calculated frosts and ices, Horizontal lines denote the average range of the two bands observed in Mariner spectra. Vertical lines then show the corresponding grain size.

Figure 10: a) Calculated reflectance of CO_2/H_2O mixes. b) Calculated reflectance of CO_2/dust mixes.

Figure 11: Spectrum number 134 (solid) compared with the calculated mixture of $C0_2$ at a 1cm grain size and 0.2% H_20 at 50 μm grain size from Fig. 10a.

Figure 12: Linear mixes of spectrum 134 with the average ground spectrum. a) 55%-134, 45%-ground (dotted) compared to spectrum 127 (solid). b) 80%-134, 20%-ground (dotted) compared to spectrum 148 (solid).

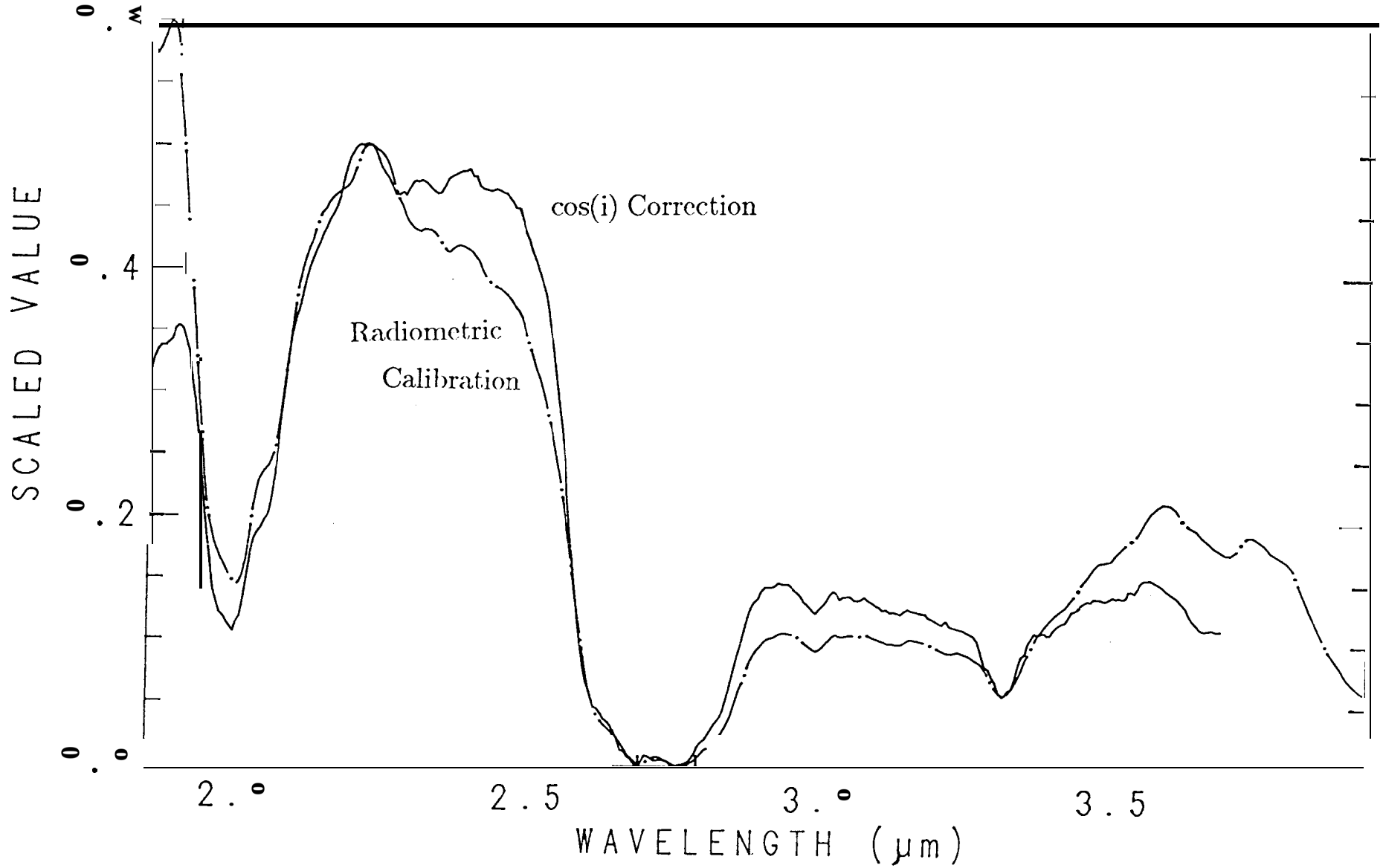
SCALED VALUE
0.6
0.4
0.2
0.0
cos(i) Correction
Radiometric
Calibration
2.0
2.5
3.0
3.5
WAVELENGTH (μm)

FIGURE 1

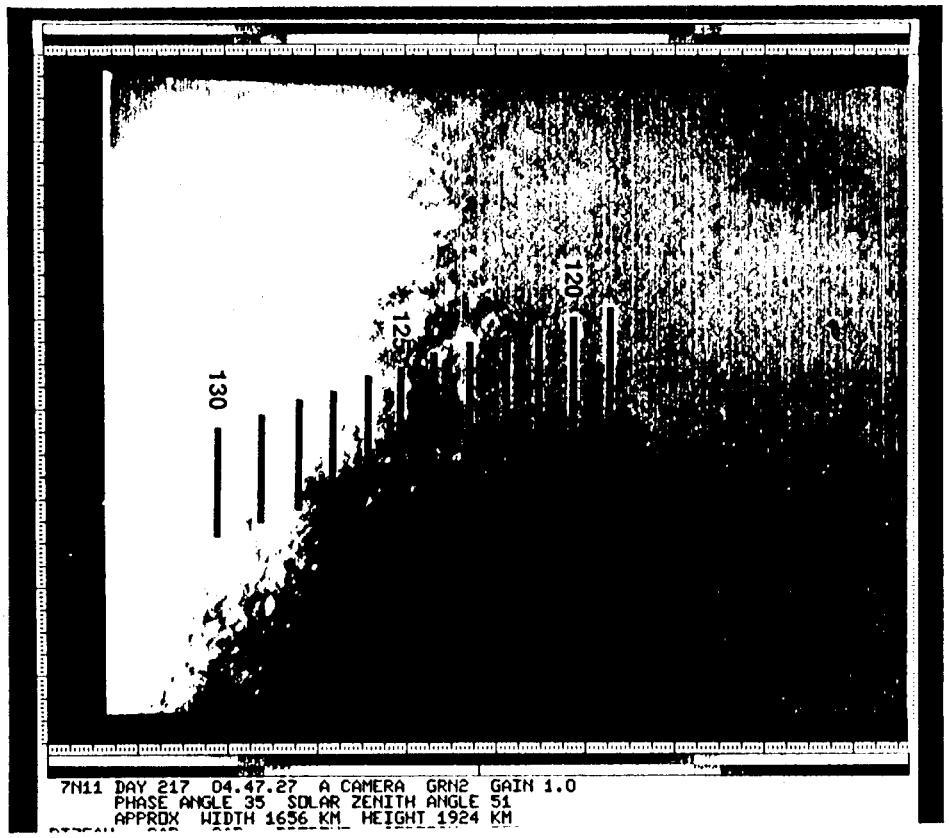

FIGURE 2a

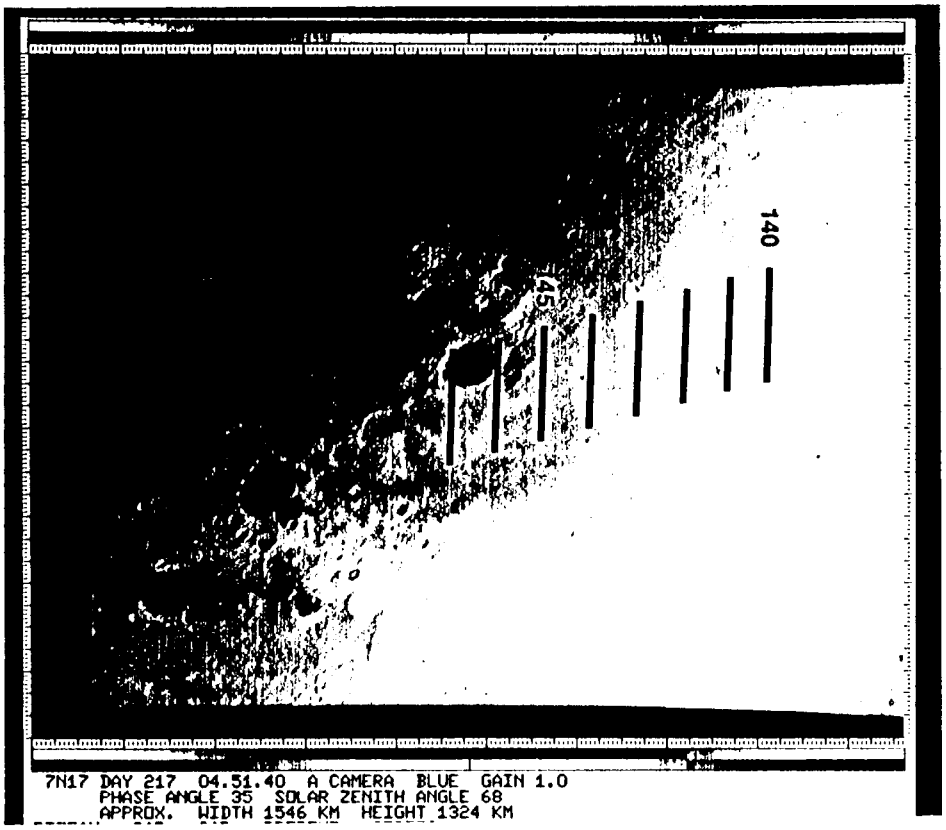

FIGURE 2b

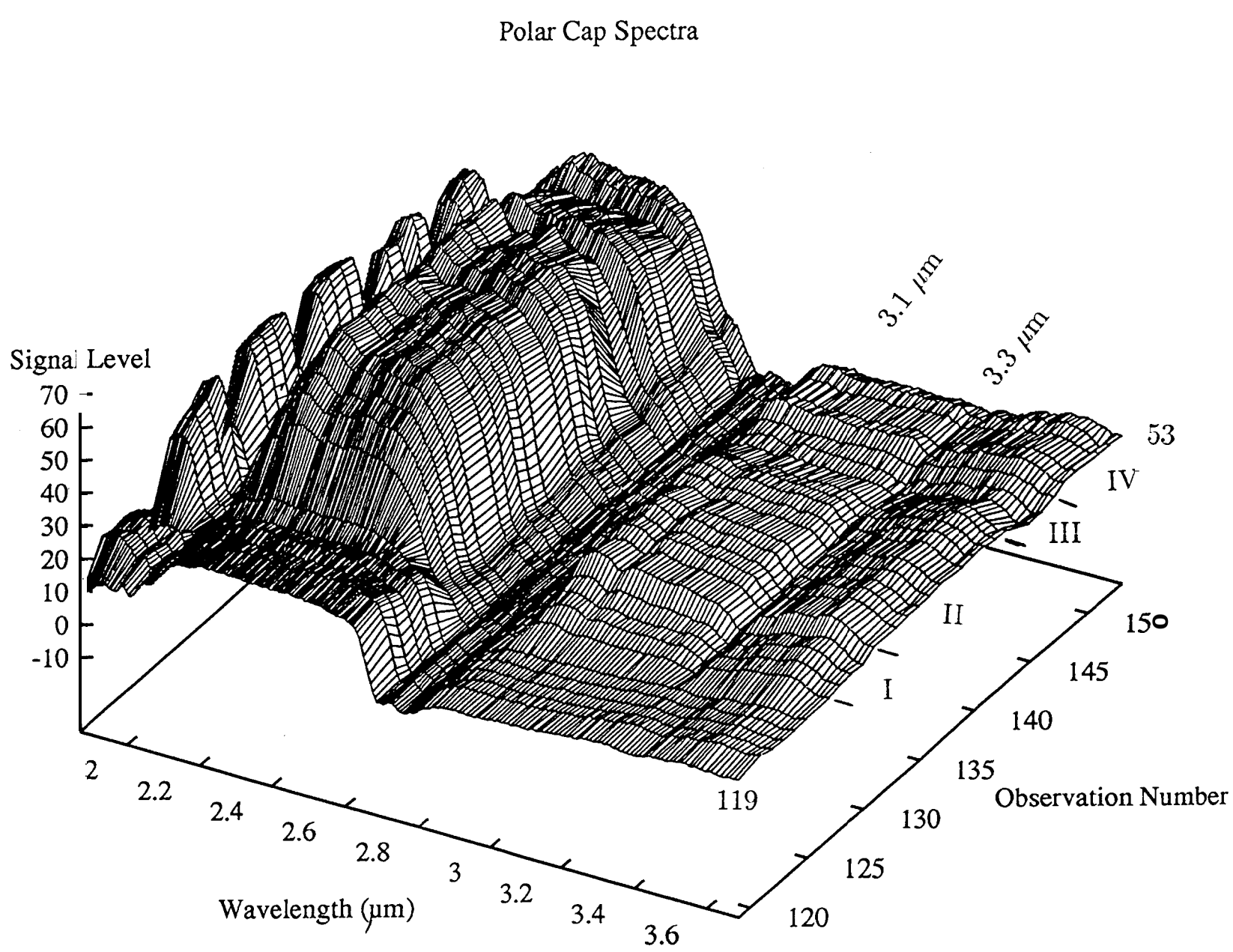
Polar Cap Spectra
Signal Level
70
60
50
40
30
20
10
0
-10
2
2.2
2.4
2.6
2.8
3
3.2
3.4
3.6
Wavelength (μm)
3.1 μm
3.3 μm
53
IV
III
II
I
119
120
125
130
135
140
145
150
Observation Number

FIGURE 3

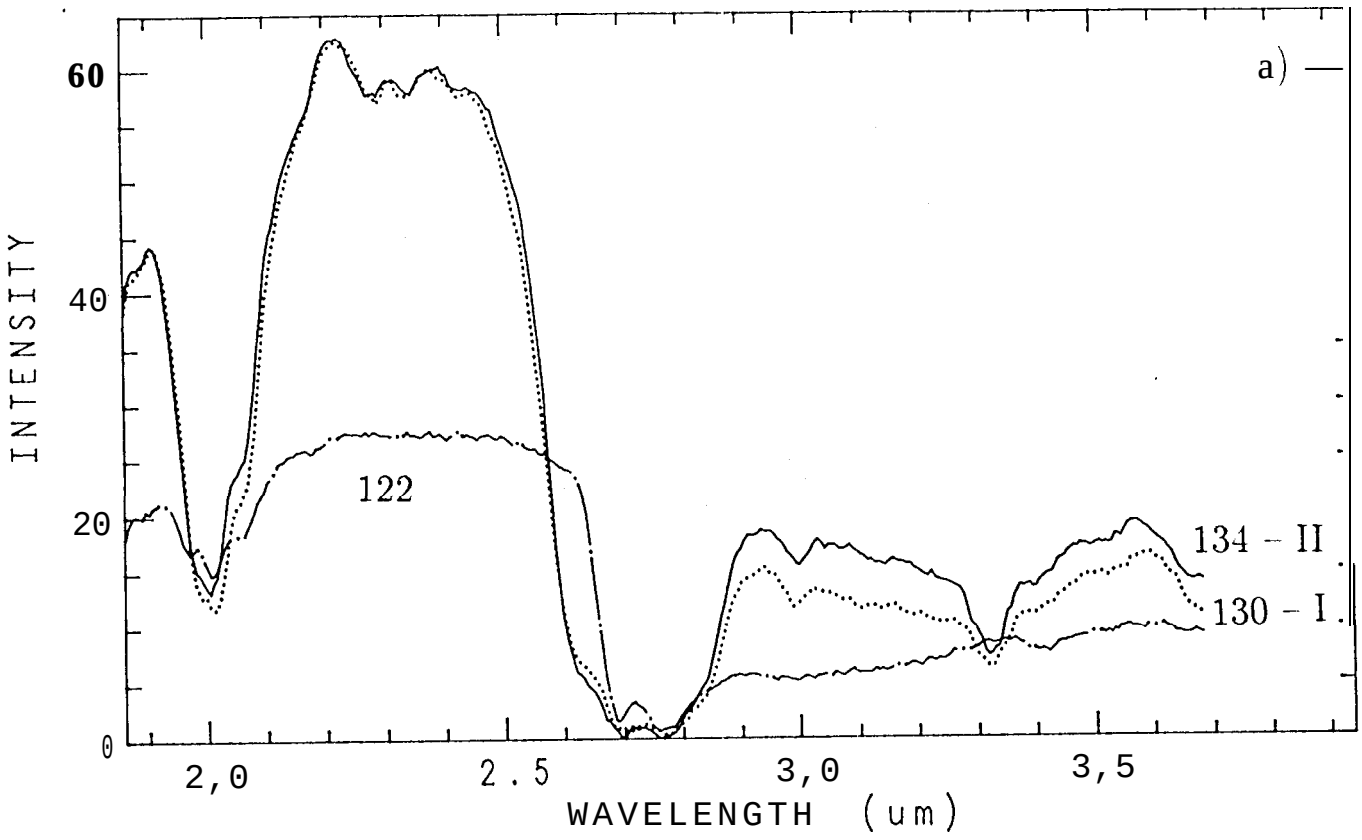
a)
60
40
20
0
INTENSITY
122
134 – II
130 – I
2,0
2.5
3,0
3,5
WAVELENGTH (um)

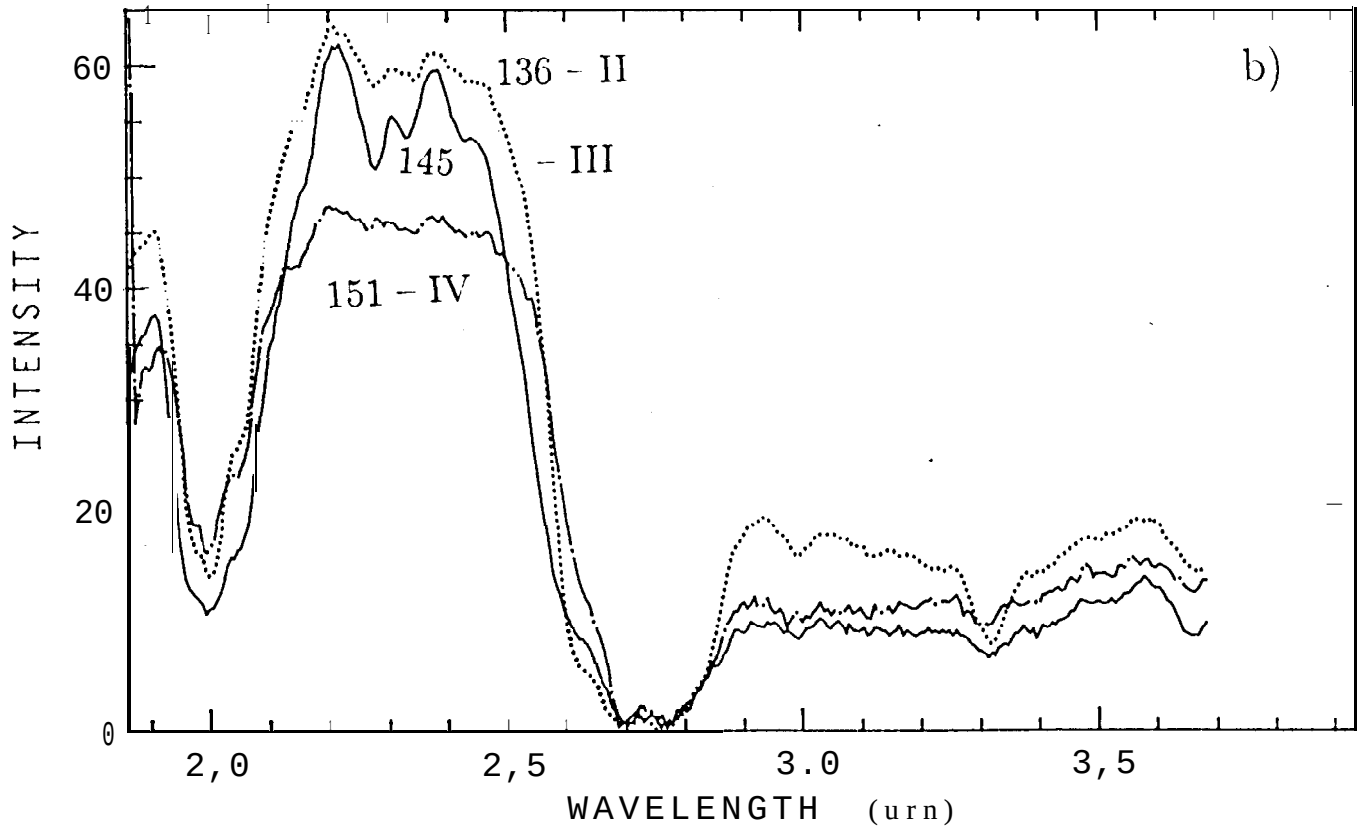
b)
60
40
20
0
INTENSITY
136 – II
145
– III
151 – IV
2,0
2,5
3.0
3,5
WAVELENGTH (urn)

FIGURE 4

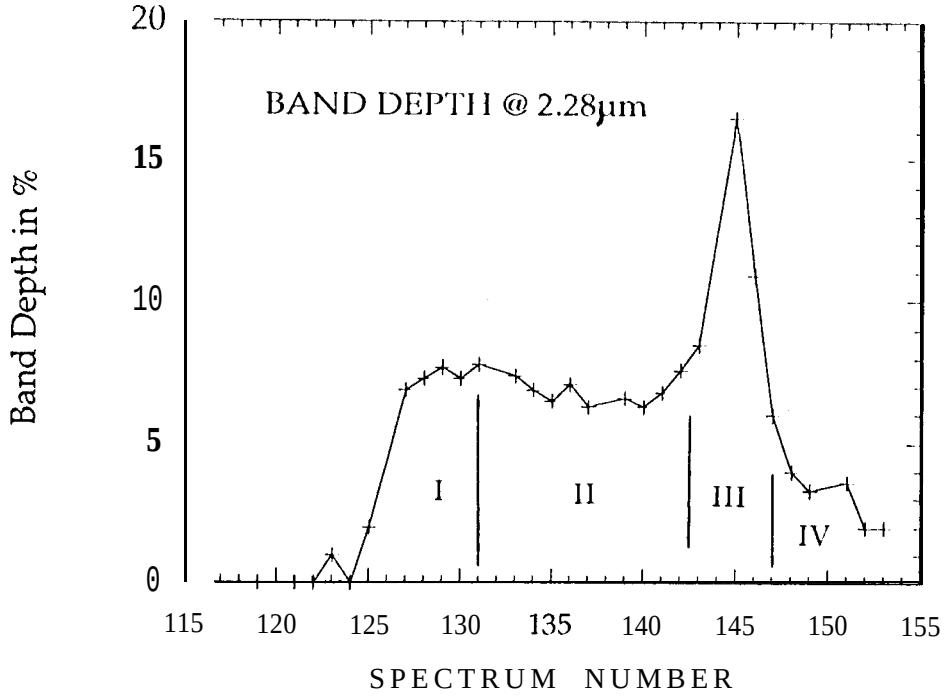

FIGURE 5

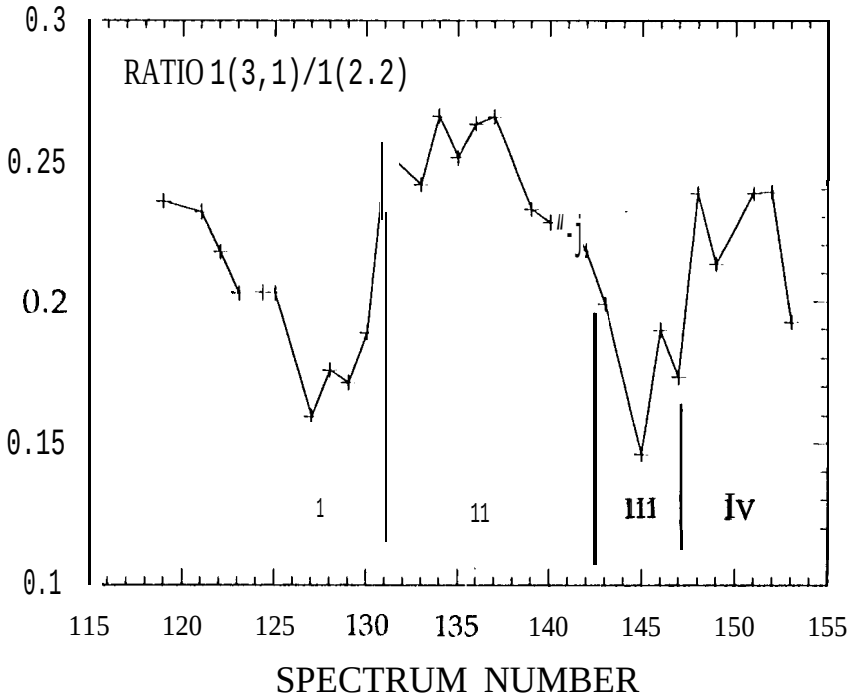

FIGURE 6

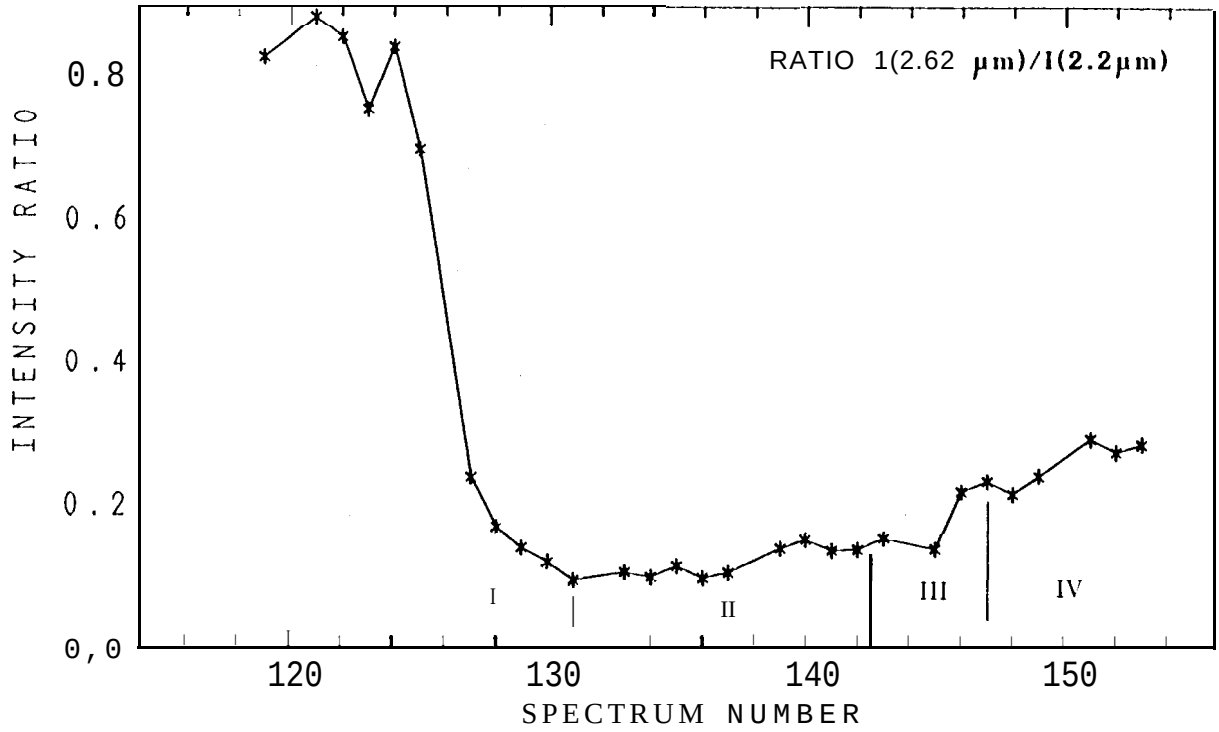

FIGURE 7

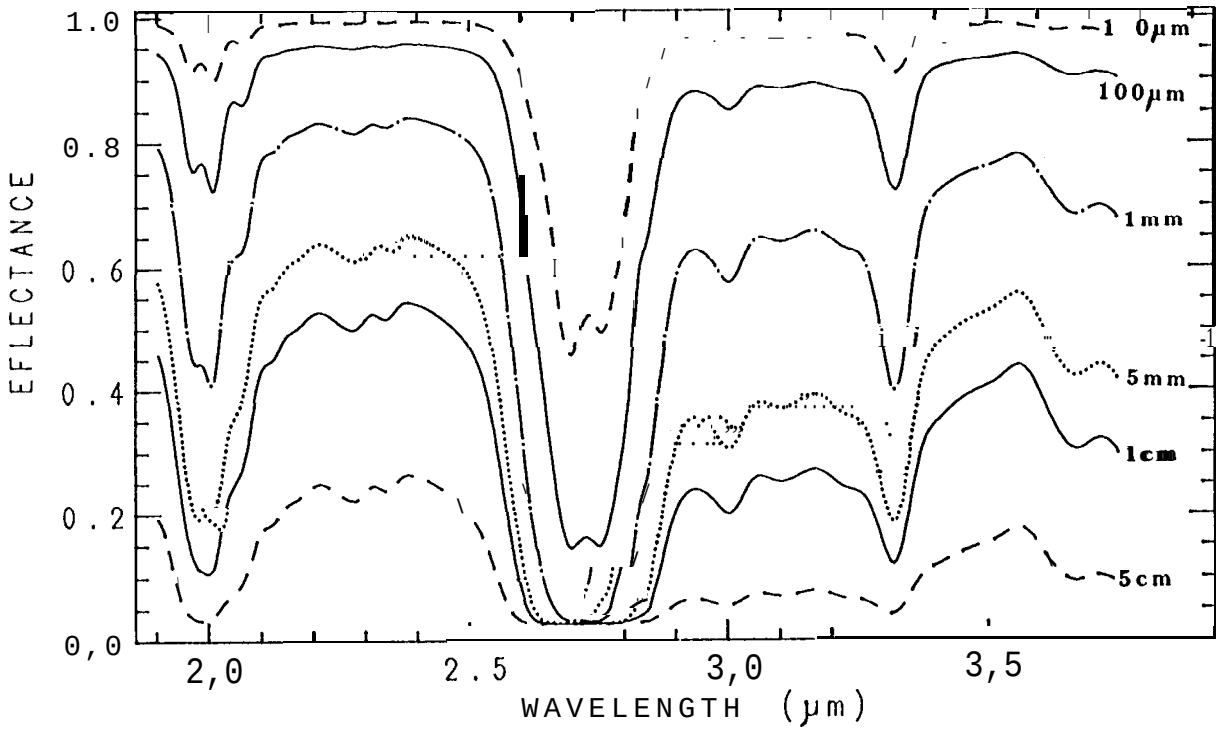

FIGURE 8

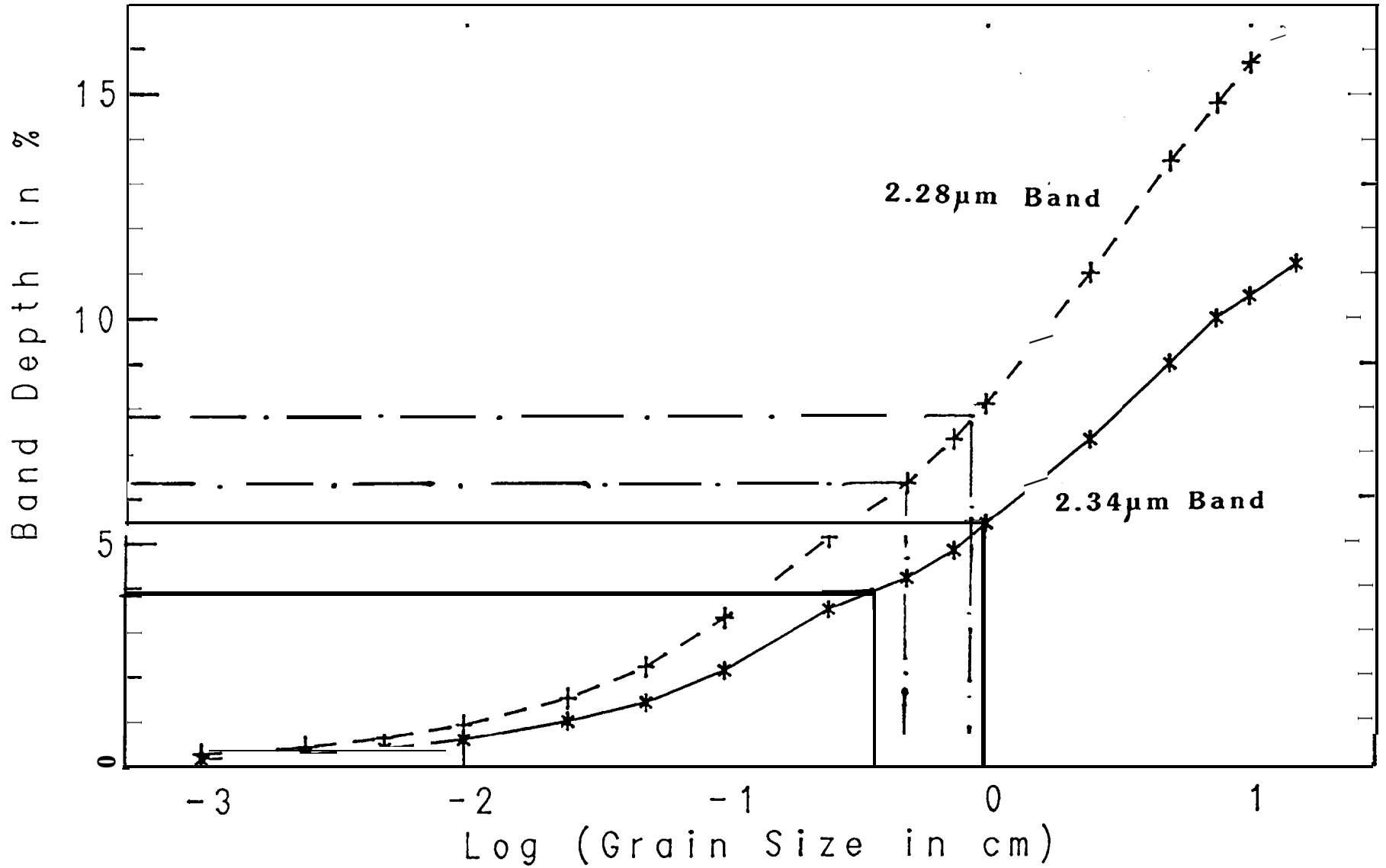
Band Depth in %
15
10
5
0
2.28µm Band
2.34µm Band
-3
-2
-1
0
1
Log (Grain Size in cm)

FIGURE 9

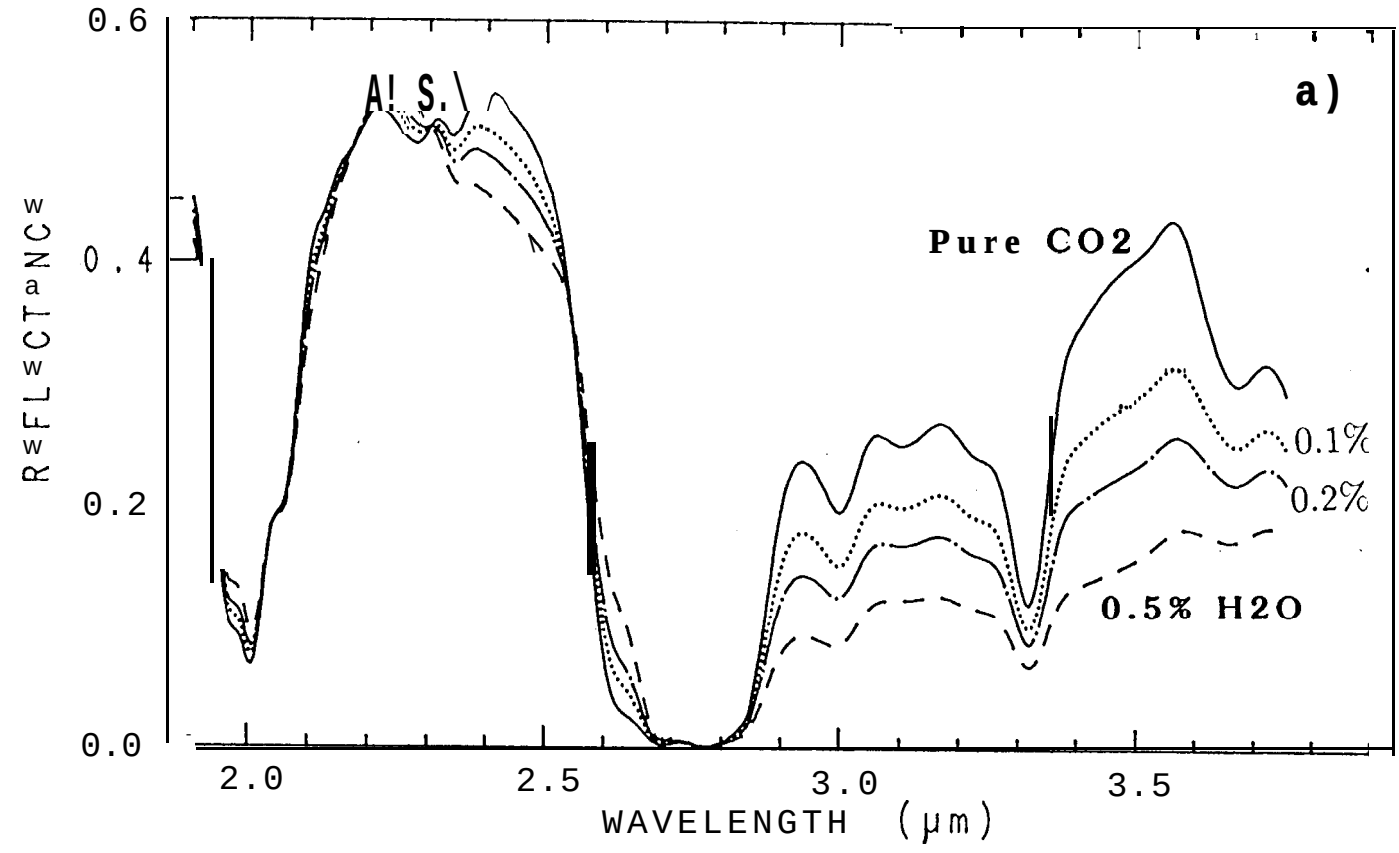
a)
A! S.
Pure CO2
0.1%
0.2%
0.5% H2O
0.6
0.4
0.2
0.0
2.0
2.5
3.0
3.5
WAVELENGTH (μm)

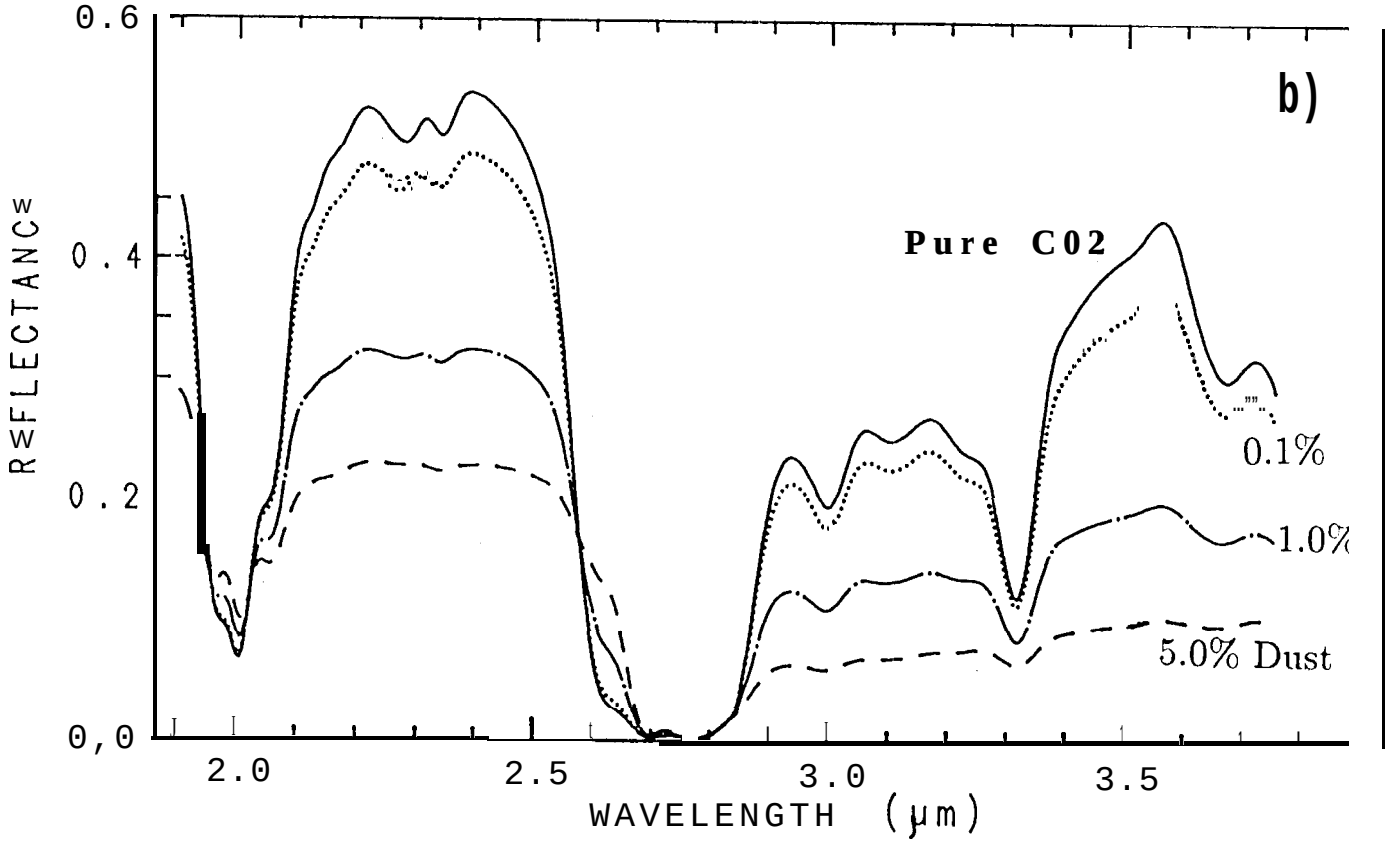
b)
Pure C02
0.1%
1.0%
5.0% Dust
0.6
0.4
0.2
0,0
2.0
2.5
3.0
3.5
WAVELENGTH (μm)

FIGURE 10

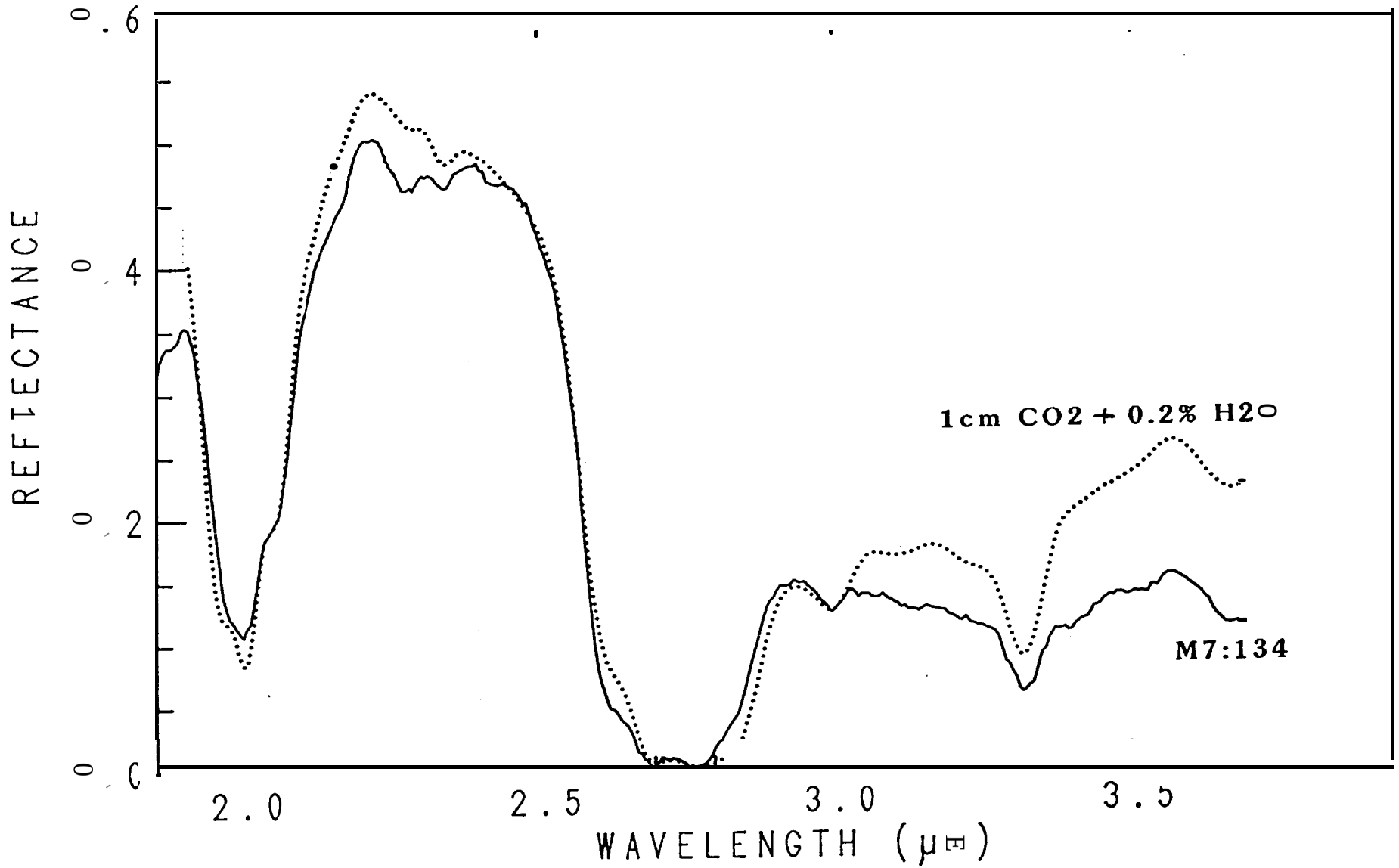
REFLECTANCE
0.6
0.4
0.2
0.0
2.0
2.5
3.0
3.5
WAVELENGTH (μm)
1cm CO2 + 0.2% H2O
M7:134

FIGURE 11

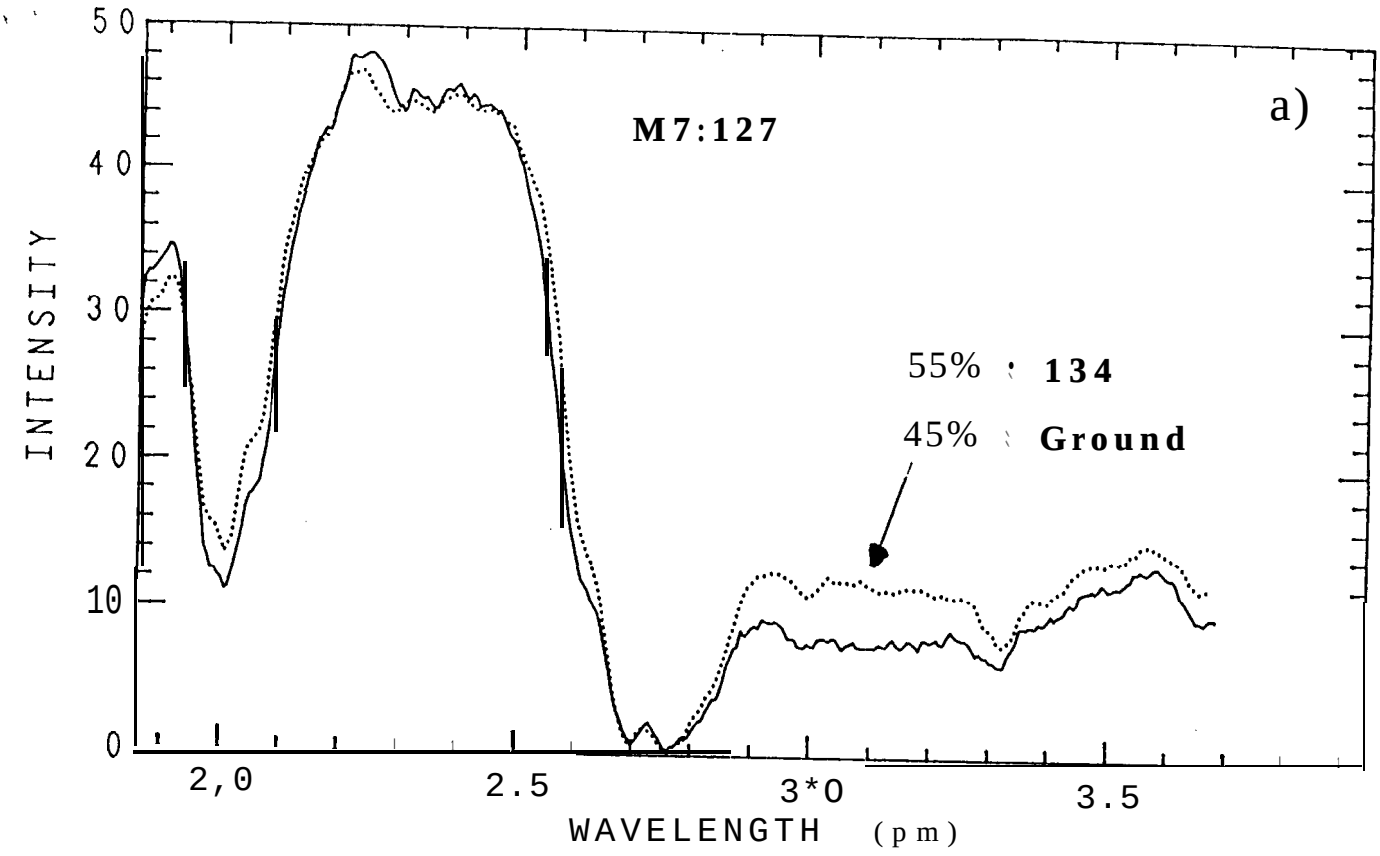
a)
M7:127
55% : 134
45% : Ground
INTENSITY
50
40
30
20
10
0
2,0
2.5
3*0
3.5
WAVELENGTH (pm)

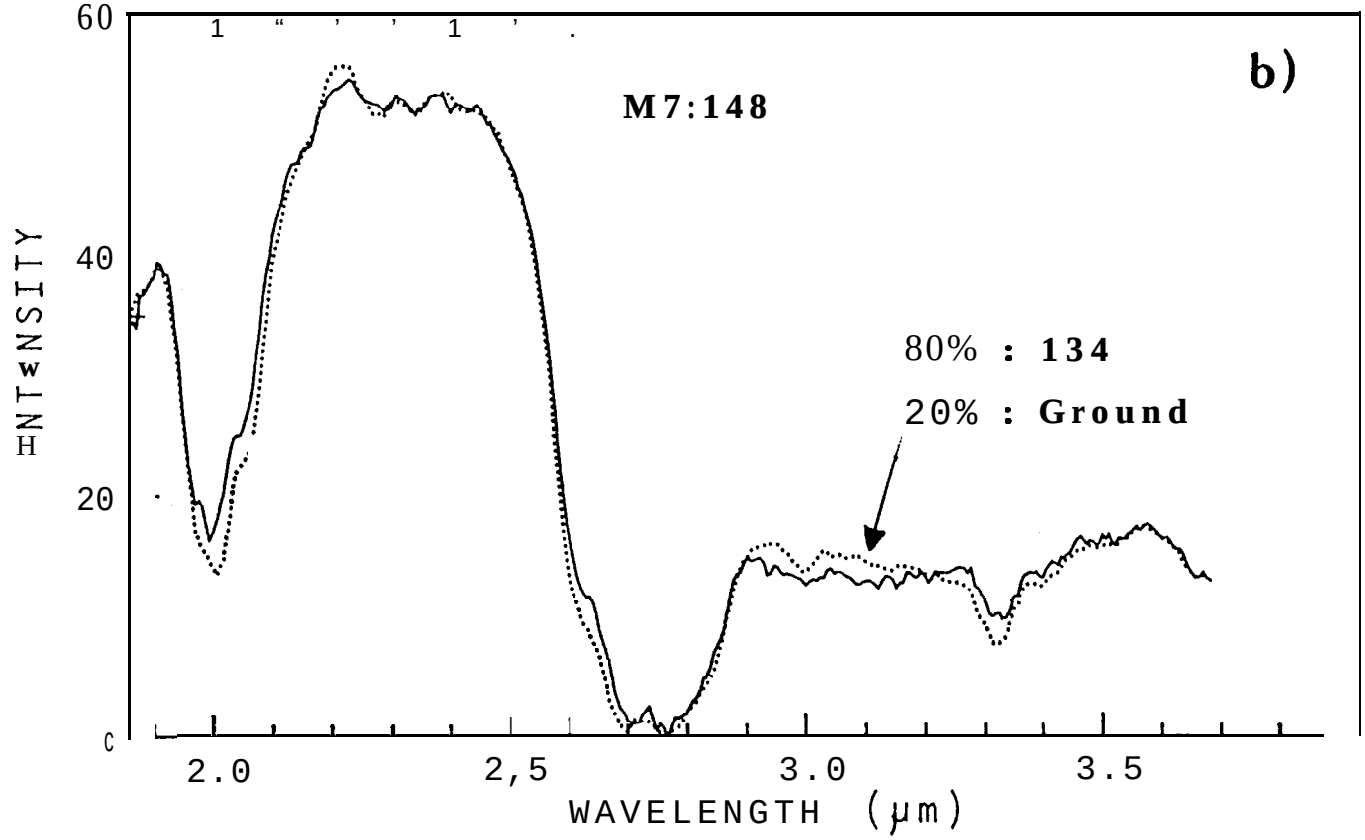
b)
M7:148
80% : 134
20% : Ground
INTENSITY
60
40
20
0
2.0
2,5
3.0
3.5
WAVELENGTH (μm)

FIGURE 12